

String effects in the 3d gauge Ising model

M. Caselle^a, M. Hasenbusch^b and M. Panero^a

^a *Dipartimento di Fisica Teorica dell'Università di Torino and I.N.F.N.,
via P.Giuria 1, I-10125 Torino, Italy*

e-mail: caselle@to.infn.it panero@to.infn.it

^b *NIC/DESY Zeuthen, Platanenallee 6, D-15738 Zeuthen, Germany*

e-mail: Martin.Hasenbusch@desy.de

Abstract

We compare the predictions of the effective string description of confinement with a set of Montecarlo data for the 3d gauge Ising model at finite temperature. Thanks to a new algorithm which makes use of the dual symmetry of the model we can reach very high precisions even for large quark-antiquark distances. We are thus able to explore the large R regime of the effective string. We find that for large enough distances and low enough temperature the data are well described by a pure bosonic string. As the temperature increases higher order corrections become important and cannot be neglected even at large distances. These higher order corrections seem to be well described by the Nambu-Goto action truncated at the first perturbative order.

1 Introduction

In these last years a lot of efforts have been devoted to extract the interquark potential from lattice gauge theories (LGT's) looking at the expectation values of Wilson loops or Polyakov loop correlators in Montecarlo simulations. Besides the important goal of obtaining reliable values of physical observables like the string tension, these simulations also allow to study the physical nature of the potential. In particular, a very interesting issue is the so called “string picture” of the interquark potential: quark and antiquark linked together by a thin fluctuating flux tube [1].

The standard approach to study this problem is to look at the finite size effects due to quantum string fluctuations, which, in finite geometries, give measurable contributions to the interquark potential. This approach traces back to the seminal work of Lüscher, Symanzik and Weisz [2] and has interesting connections with the conformal field theory (CFT) approach of two-dimensional models developed in the eighties [3, 4].

The major problem in trying to use these finite size corrections to obtain information on the underlying effective string is that very high precision estimates of the interquark potential are needed. Such a precision is very hard to reach with standard algorithms, in particular if one is interested in the large distance regime where the effective string should show up.

This led us in the past years to concentrate on the simplest non-trivial LGT, namely the 3d gauge Ising model for which, thanks to the dual transformation, new and very powerful algorithms can be constructed and very high precisions can be reached within a reasonable amount of CPU-time even for large distance interquark potentials. Following this line we found convincing evidences for the existence of a bosonic type effective string theory in the 3d gauge Ising model both in the case of the Wilson loop geometry [5] (fixed boundary conditions (bc) in both directions) and of the interface geometry [6] (periodic bc in both directions). This paper deals with the third remaining case, namely that of the Polyakov loop correlators, which corresponds to a mixed geometry (fixed b.c in one direction and periodic b.c. in the other direction). A preliminary account of the present study recently appeared in [7]. Here we complete the analysis using a new algorithm which fully exploits the power of dual transformations, leading to a gain of more than one order of magnitude in precision with respect to [7]. Thanks to this higher resolution

we are now able to explore in greater detail the fine structure and the higher order corrections of the underlying effective string theory. This is the main goal of the present paper.

While studying the Ising model allows a very careful control of all possible sources of systematic errors and a very precise study of the fine details of the underlying effective string, it remains an open problem to see if the results obtained are particular features of the gauge Ising model only or have a more general validity and can be extended also to non-abelian LGT which are more interesting from a physical point of view.

Last year, an important progress was made in this direction, thanks to a new, powerful, algorithm proposed by Lüscher and Weisz in [8]. With such an algorithm an exponential reduction of statistical errors of Polyakov loop correlators can be obtained with no need of dual transformations. Hence it can be used for any non-abelian LGT, thus allowing to study the possible existence of string corrections in a much wider set of models. In particular it was recently used by the same authors in [9] to study the $SU(3)$ theory both in $(2+1)$ and $(3+1)$ dimensions. In both cases they found again a good agreement with the predictions of the free bosonic effective string theory.

Thanks to this relevant progress it is now possible to address the important issue of the string universality, i.e. to compare the properties of the effective strings underlying different LGT's. It is by now clear that for large enough distances (and low enough temperatures in the case of Polyakov loop correlators) one always finds the same asymptotic theory, i.e. the free bosonic effective theory originally studied in [2]. However for shorter distances and/or higher temperatures, terms of higher order (typically self-interaction terms or boundary-type contributions) which are present in the string action start to give measurable corrections and can be detected and studied.

In this respect Polyakov loop correlators turn out to be a perfect tool to study these effects, since as the temperature increases these higher order corrections become rather large even for large interquark distances, i.e. in a regime in which other possible sources of corrections (say, for instance, the perturbative one gluon exchange contribution in $SU(3)$) are under control or negligible.

Thanks to this fact and to the relevant precision of our simulations we are able to precisely observe the deviations with respect to the free bosonic string

predictions, and we can see that, as expected, they increase in magnitude as the temperature increases. We shall also show that these corrections are well described (with some cautionary remarks discussed in sect. 4 and 5 below) by a Nambu-Goto type string action, truncated at the first perturbative order.

This paper is organized as follows. In sect. 2 we shall discuss some general results concerning the effective string description of the interquark potential. We shall introduce both the bosonic string and the self-interaction terms induced by the Nambu-Goto string. We shall then discuss the corresponding finite size corrections. We made an effort to make this section as self-contained as possible, so as to allow the reader to follow all the steps of the derivation. In sect. 3 we shall give a few general information on the 3d gauge Ising model, on the algorithm that we used to simulate the model, and we shall also describe in some detail the simulations that we performed. In sect. 4 we shall discuss our results. Finally sect. 5 will be devoted to some concluding remarks and to a comparison with the analogous results obtained in $SU(3)$ in [9].

2 Theory

As mentioned in the introduction, Polyakov loops naturally arise if one studies finite temperature LGT. Thus we shall begin this section with a brief summary of known results on finite temperature LGT (sect. 2.1). This will also allow us to fix notations and conventions. Next we shall address the issue of finite size corrections, following two complementary paths. First we shall discuss them in full generality, without resorting to any specific string model, but simply exploiting the quantum field theory implications of the roughening transition (sect. 2.2), using some general results of Conformal Field Theory (sect. 2.3) and the exact solution of the CFT of a free boson (sect. 2.4). This approach is very powerful but it allows no insight in possible higher order corrections due to the self-interaction of the string. To this end a precise choice of the effective string model (i.e. the precise form of world-sheet Lagrangian of the underlying string) is needed. We shall address this point in sect. 2.5, studying the simplest possible string (the natural generalization of the free bosonic CFT) i.e. the Nambu-Goto string. Next in sect. 2.6 we shall outline the implications of this choice for our understanding of

the deconfinement transition. Finally we close this theoretical introduction by addressing the important issue of the range of validity of the effective string picture (sect. 2.7).

2.1 Finite temperature gauge theories: general setting and notations

The partition function of a gauge theory in d spacetime dimensions with gauge group G regularized on a lattice is

$$Z = \int \prod dU_l(\vec{x}, t) \exp\{-\beta \sum_p \text{Re Tr}(1 - U_p)\} \quad , \quad (1)$$

where $U_l(\vec{x}, t) \in G$ is the link variable at the site $(\vec{x}, t) = (x_1, \dots, x_{d-1}, t)$ in the direction l and U_p is the product of the links around the plaquette p .

Let us call N_t (N_s) the lattice size in the time (space) direction (we assume for simplicity N_s to be the same for all the space directions). Lattice simulations with non-zero temperature are obtained by imposing periodic boundary conditions in the time direction. A $(N_s)^{d-1}N_t$ lattice can then be interpreted as representing a system of finite volume $V = (N_s a)^{d-1}$ at a finite temperature $T = 1/L = 1/N_t a$ where a is the lattice spacing. To simplify notations we shall fix from now on the lattice spacing to be 1 and neglect it in the following.

The order parameter of the finite temperature deconfinement transition is the Polyakov loop, *i.e.* the trace of the ordered product of all time links with the same space coordinates; this loop is closed owing to the periodic boundary conditions in the time direction:

$$P(\vec{x}) = \text{Tr} \prod_{z=1}^{N_t} U_t(\vec{x}, z) \quad . \quad (2)$$

The vacuum expectation value of the Polyakov loop is zero in the confining phase and acquires a non-zero expectation value in the deconfined phase. The value $\beta_c(T)$ of this deconfinement transition is a function of the temperature, and defines a new physical observable T_c . The inverse of this function gives for each value of β the lattice size in the time direction (which we shall call in the following $N_{t,c}(\beta)$) at which the model undergoes the deconfinement transition.

The interquark potential can be extracted by looking at the correlations of Polyakov loops in the confined phase. The correlation of two loops $P(x)$ at a distance R and at a temperature $T = 1/L = 1/N_t$ is given by

$$G(R) \equiv \langle P(x)P^\dagger(x+R) \rangle \equiv e^{-F(R,L)} \quad , \quad (3)$$

where the free energy $F(R, L)$ is expected to be described, as a first approximation, by the so called “area law”:

$$F(R, L) \sim F_{cl}(R, L) = \sigma LR + k(L) \quad , \quad (4)$$

where σ denotes the string tension¹ and $k(L)$ is a non-universal constant depending only on L . The meaning of the index cl refers to the fact that (as will be discussed below) this should be considered as a “classical” result, which neglects quantum fluctuations.

In the following we shall mainly study the combination

$$Q_0(R, L) \equiv F(R+1, L) - F(R, L) \equiv \log \left(\frac{G(R)}{G(R+1)} \right) \quad (5)$$

in which the non-universal constant cancels out.

The observable (3) is similar to the expectation value of an ordinary Wilson loop except for the boundary conditions, which are in this case fixed in the space directions and periodic in the time direction. The resulting geometry is that of a cylinder, which is topologically different from the rectangular geometry of the Wilson loop.

2.2 The roughening transition and the effective string

Eq.(4) correctly describes the Polyakov loop correlators only in the strong coupling phase. As it is well known the confining regime of a generic lattice gauge theory consists in general of two phases: the strong coupling phase and the rough phase. These two phases are separated by the roughening transition where the strong coupling expansion for the Polyakov loop correlator (as well as that for the Wilson loop or the interface) ceases to converge [10, 2].

¹In the following, when needed, we shall also explicitly write the dependence of the string tension on the finite temperature T and the coupling β as $\sigma(T)$ or $\sigma(T, \beta)$ depending on the case

These two phases are related to two different behaviors of the quantum fluctuations of the flux tube around its equilibrium position [2]. In the strong coupling phase, these fluctuations are massive, while in the rough phase they become massless and hence survive in the continuum limit. The inverse of the mass scale of these fluctuations ² can be considered as a new correlation length of the model. It is exactly this new correlation length which goes to infinity at the roughening point and induces the singular behavior of the strong coupling expansion.

In the rough phase the flux-tube fluctuations can be described by a suitable two-dimensional massless quantum field theory, where the fields describe the transverse displacements of the flux tube. The common lore is that this QFT should be the effective low energy description of some fundamental string theory (this is the reason for which this QFT is often called “effective string theory” and the finite size contributions it induces are usually named “string corrections”)³. It is expected to be very complicated and to contain in general non-renormalizable interaction terms [2]. However, exactly because these interactions are non-renormalizable, their contribution is expected to be negligible in the infrared limit (namely for large quark separation) [12]. In this infrared limit the QFT becomes a conformal invariant field theory (CFT) [4].

From the general theory of CFT’s we immediately see that there are two important signatures which, if detected, could validate the whole picture, and which could be in principle observed in numerical simulations.

- (1) The massless quantum fluctuations delocalize the flux tube which acquires a nonzero width, which diverges logarithmically as the interquark distance increases [13, 14].
- (2) These quantum fluctuations give a non-zero contribution to the interquark potential, which is related to the partition function of the above 2d QFT. Hence if the 2d QFT is simple enough to be exactly solvable (and this is in general the case for the CFT in the infrared

²Notice that this scale is completely different from the glueball mass scale.

³Notice however that the existence of such an underlying fundamental string theory is not a mandatory requirement to justify the results that we shall discuss below. Any alternative mechanism (see for instance [11]) which could induce a fluctuating flux tube description for the interquark potential works equivalently well.

limit) also these contributions can be evaluated exactly. They show up as finite size corrections to the interquark potential.

It is this last signature which is the best suited to be studied by numerical method and which we shall address in the following section.

2.3 Finite Size Effects: general discussion

As mentioned above, the pure area law is inadequate to describe the Polyakov loop correlator in the rough phase and must be multiplied by the partition function of the 2d QFT describing the quantum fluctuations of the flux tube which in the infrared limit becomes a 2d CFT. Let us call $Z_q(R, L)$ the partition function of such CFT on the cylinder (the open ends of the cylinder being the two Polyakov loops). Then eq. (4) in the rough phase becomes:

$$\langle P(x)P^\dagger(x+R) \rangle = e^{-F_{cl}(R,L)} Z_q(R, L) \quad . \quad (6)$$

Defining the free energy of quantum fluctuations as

$$F_q(R, L) = -\log Z_q(R, L) \quad ,$$

we find for the free energy

$$F(R, L) \sim F_{cl}(R, L) + F_q(R, L) = \sigma LR + k(L) - \log Z_q(R, L) \quad . \quad (7)$$

By using standard CFT's [4] methods we can study the behavior of $F_q(R, L)$ as a function of R and L in a general way. Indeed any two dimensional CFT is completely described once the conformal anomaly c , the operator content h_i and the operator product algebra (or the fusion algebra which equivalently encodes all the fusing properties of the CFT) are given. Then it is easy to show that $F_q(R, L)$ only depends on the adimensional ratio⁴ $z = 2R/L$. It is possible to give asymptotic expressions for $F_q(R, L)$ in the $z \gg 1$ and $z \ll 1$ regimes:

$z \gg 1$ [15]:

$$F_q(R, L) \simeq -\tilde{c} \frac{\pi R}{6L} \quad , \quad (8)$$

⁴the factor of 2 in the definition of z is a consequence of the asymmetry in the boundary conditions.

where $\tilde{c} = c - 24h_{min}$ is the effective conformal anomaly [16]; h_{min} is the lowest conformal weight of the physical states propagating along the cylinder. In the case of unitary CFT's $h_{min} = 0$ (unless special boundary conditions are chosen) and \tilde{c} coincides with the conformal anomaly c ;

$z \ll 1$ [17]:

$$F_q(R, L) \simeq -\hat{c} \frac{\pi L}{24R} \quad , \quad (9)$$

where $\hat{c} = c - 24h_{\alpha, \beta}$ and $h_{\alpha, \beta}$ is the lowest conformal weight compatible with the boundary conditions α and β at the two open ends of the cylinder. In the case of an unitary CFT and fixed bc we have again $h_{\alpha, \beta} = 0$.

If the CFT is exactly solvable, namely if the whole operator content is known, one can explicitly write the free energy for all values of z , which smoothly interpolates between the two asymptotic behaviors.

An important role in this construction is played by the modular transformations. All the partition functions can be written as power expansions in $q = \exp(2\pi i\tau)$, with $\tau = iz$ for Polyakov loop correlations (notice that $\tau = i\frac{R}{L}$ if one studies Wilson loops). Modular transformations allow to extend these expansions in the whole τ plane. In particular we shall be interested, in the following, in the $\tau \rightarrow -1/\tau$ transformation.

In the Wilson loop case, this transformation is a symmetry, because it exchanges R and L . We can use this symmetry by choosing for instance $L \geq R$, and $\tau = iL/R$. With this choice L plays the role of a time-like extent and the interquark potential $V(R)$ we want to extract from the data is defined in the limit: $V(R) = \lim_{L \rightarrow \infty} F(R, L)/L$. A similar symmetric situation occurs if one studies the behavior of the interface tension (see for instance [6]).

In the Polyakov loop case, the situation is completely different: L and R have a different meaning and the modular transformation $\tau \rightarrow -1/\tau$ allows us to move from the region in which $2R > L$ to that in which $2R < L$. What is new is that, due to the modular transformation, in these two regions the string corrections have, as we have seen above, different functional forms. While in the region in which $2R < L$ the dominant contribution is, like in the Wilson loop case, of the type $1/R$, in the region in which $2R > L$ the dominant contribution is proportional to R , and acts as a finite size correction of the string tension. This behavior will play a major role in the following.

2.4 The simplest case: the free bosonic string

The simplest possible choice for the CFT which should describe the effective string in the infrared limit is to assume that the $d - 2$ fields which describe the transverse displacement of the flux tube are $d - 2$ free non-interacting bosons. We shall denote in the following this approximation of F_q with the notation F_q^1 and the corresponding partition function as Z_1 ⁵.

With abuse of language this choice is usually referred to as the “bosonic string” model. Notice however that this model, being only an effective long range description, could well be related to a wide class of wildly interacting (and not necessarily bosonic) string theories. Besides being the simplest choice this model is very important for at least three reasons:

- 1] In the framework of the interface physics this QFT is known as “*capillary wave model*” and has received in the past years impressive confirmations in a set of studies of different models belonging to the Ising universality class (see for instance ref. [6] and references therein).
- 2] Historically it was the first to be studied in QCD. The so called “Lüscher term” actually is nothing but the dominant contribution of this bosonic string correction in the $2R < L$ limit.
- 3] It has been recently observed that it well describes the finite size corrections of the interquark potential in SU(3) LGT both extracted from Wilson loops [18] and from Polyakov loops correlators [9] and also in SU(N) LGT with $N \neq 3$ [19] (see also the analysis of [20]).

Notwithstanding being the simplest one, this CFT is all the same highly non-trivial. In particular, as we shall see in detail in sect. 3, the peculiar choice of lattice sizes which is usually made in standard lattice simulations require that one takes into account the *whole* functional form of $F_q^1(R, L)$, and not only the dominant contributions discussed in eq.s (8) and (9). This is indeed one of the main points of this paper and we shall discuss it in detail in sect. 4 when comparing our predictions with the numerical simulations.

The whole functional form of $F_q^1(R, L)$ can be evaluated by a suitable regularization of the Laplacian determinant (or alternatively by summing

⁵The rationale behind this choice is that we think of F_q^1 as the first term in the expansion of F_q in powers of $(\sigma RL)^{-1}$. We shall address below the second term of this expansion which we shall denote as F_q^{NLO} .

over the whole set of states of the Virasoro algebra). This result has a rather long history: it was discussed for the first time in 1978 by M. Minami in [21]. It was then reobtained in ref.s [22, 23] and with a different approach in ref. [24]. Here, we only report the result, which for a d dimensional gauge theory (i.e. $d - 2$ bosonic fields) is:

$$F_q^1(R, L) = (d - 2) \log(\eta(\tau)) \quad ; \quad -i\tau = \frac{L}{2R} \quad , \quad (10)$$

where η denotes the Dedekind eta function:

$$\eta(\tau) = q^{\frac{1}{24}} \prod_{n=1}^{\infty} (1 - q^n) \quad ; \quad q = e^{2\pi i \tau} \quad , \quad (11)$$

and R is the distance between the two Polyakov loops.

We list below for completeness the power expansions in the two regions:

$$2R < L$$

$$F_q^1(R, L) = \left[-\frac{\pi L}{24R} + \sum_{n=1}^{\infty} \log(1 - e^{-\pi n L/R}) \right] (d - 2) \quad , \quad (12)$$

$$2R > L$$

$$F_q^1(R, L) = \left[-\frac{\pi R}{6L} + \frac{1}{2} \log \frac{2R}{L} + \sum_{n=1}^{\infty} \log(1 - e^{-4\pi n R/L}) \right] (d - 2) \quad . \quad (13)$$

These are the expressions that we shall compare in sect. 4 with our Montecarlo data. Notice, as a side remark, that for any practical purpose it is enough to truncate the infinite sums which appear in eq.s (12) and (13) to the first two or three terms. The errors obtained in this way (if one remains inside the regions of validity of the two expansions: $z < 1$ for eq.(12) and $z > 1$ for eq.(13)) are much smaller than the uncertainties of the numerical estimates.

2.5 The Nambu-Goto string

The approach discussed in the previous sections is very general. It shows that at large enough interquark distance, the finite size corrections to the potential are independent of the fine structure details of the effective string model

and only depend on the choice of boundary conditions, on the number of transverse dimensions and on the geometry of the observable used to extract the potential. This *universality* of the string correction was already observed by Lüscher, Symanzik and Weisz in their original papers [2] and remains the nicest feature of the effective string approach to the interquark potential. However, it is clear that along this way we have no hope to predict the effect (or even simply check the existence) of higher order corrections due to the self-interaction of the string. These self-interaction terms are expected to play a role in the intermediate region, before the asymptotic regime of the pure free bosonic CFT is reached. Notice however that there is no sharp separation between these two regimes, and the border between them only depends on the resolution of the data used to test the predictions. Precise enough data could allow to detect these higher order terms (if they exist) at any value of the interquark distance.

In order to study the self-interaction of the string, a precise choice of the effective string model (i.e. a precise form for the world-sheet Lagrangian of the underlying string) is needed. In this paper we shall follow the simplest possible option, which is known as the Nambu-Goto action. There are a few reasons which support this choice:

- It is the simplest and most natural generalization of the free bosonic CFT, since its action is simply given by the area of the world-sheet, with no need of additional information or degree of freedom.
- It implies a behavior of the deconfinement temperature which seems to agree rather well the simulations (see sect. 2.6 below).
- As far as we know, there is only one other case in which higher order corrections to the free effective string have been detected and studied, i.e. the finite size behavior of the interface free energy in the three dimensional Ising model [6, 25]. In this case the Montecarlo data were in perfect agreement with the predictions obtained using the Nambu-Goto action.

However it is important to stress that this is by no means the only possible choice. In fact there are several other actions which can give (at the first order to which we are addressing the problem here) the same corrections.

Besides the self-interaction type terms, one could also include in the action “boundary type” terms, like those studied in [9]. We decided in this

paper to neglect this class of higher order corrections, since they require the introduction of a free parameter which must be fitted from the data and also because here we are mainly interested in the string self-interaction terms. However we plan to address the issue of boundary correction in a forthcoming paper.

2.5.1 Finite size corrections due to the Nambu-Goto string

The major problem of the derivations that we shall discuss below is that the gauge choice that we have to make in order to be able to perform our calculations is not consistent at the quantum level. There are arguments which tell us that this anomaly should vanish at large enough distance [12], but this cannot eliminate the problem. This is the reason for which we repeatedly stressed in this paper that what we are addressing here is an *effective* string model. We are here in a completely different framework with respect to the *fundamental* string theories, for which consistence at the quantum level is mandatory.

We must think of the Nambu-Goto action as a low energy, large distance, approximation of the “true” (unknown) fundamental string theory.

This can be clarified by looking at the 3d Ising model as an example. The fundamental string is expected to describe the model at the microscopic level. The common assumption is that it should describe the behavior (and the statistics) of the surfaces contained in the strong coupling expansion of the model, as it does the free fermion field theory in the 2d case. On the contrary, the effective string theory should describe the behavior of these surfaces at a much larger distance scale, where the microscopic features become negligible and one only looks at the collective modes of the fluctuations of these surfaces which behave, as a first approximation, as free massless bosonic fields.

As anticipated above, the Nambu-Goto string action is simply given by the area of the world-sheet:

$$S = \sigma \int_0^L d\tau \int_0^R d\varsigma \sqrt{g} \ , \quad (14)$$

where g is the determinant of the two-dimensional metric induced on the world-sheet by the embedding in R^d :

$$g = \det(g_{\alpha\beta}) = \det \partial_\alpha X^\mu \partial_\beta X^\mu \ . \quad (15)$$

$(\alpha, \beta = \tau, \varsigma, \ \mu = 1, \dots, d)$

and σ is the string tension.

The reparametrization and Weyl invariances of the action (14) require a gauge choice for quantization. We choose the “physical gauge”

$$\begin{aligned} X^1 &= \tau \\ X^2 &= \varsigma \end{aligned} \quad (16)$$

so that g is expressed as a function of the transverse degrees of freedom only:

$$\begin{aligned} g &= 1 + \partial_\tau X^i \partial_\tau X^i + \partial_\varsigma X^i \partial_\varsigma X^i \\ &\quad + \partial_\tau X^i \partial_\tau X^i \partial_\varsigma X^j \partial_\varsigma X^j - (\partial_\tau X^i \partial_\varsigma X^i)^2 \\ &\quad (i = 3, \dots, d) . \end{aligned} \quad (17)$$

The fields $X^i(\tau, \varsigma)$ must satisfy the boundary conditions dictated by the problem. In our case periodic bc in one direction and Dirichlet bc in the other one:

$$X^i(0, \varsigma) = X^i(L, \varsigma); \quad X^i(\tau, 0) = X^i(\tau, R) = 0 . \quad (18)$$

It is clear that this gauge fixing implicitly assumes that the surface is a single valued function of (τ, ς) , i.e. it must not have overhangs or cuts. This is certainly not the case for the microscopic surfaces which one obtains in the strong coupling expansion. Thus this gauge fixing is just another way to state that the string that we are studying is an effective string. This point can be made more rigorous by looking at the quantum consistency of this gauge fixing. Indeed it is well known that due to the Weyl anomaly this gauge choice can be performed at the quantum level only in the critical dimension $d = 26$. However, in agreement with our picture of a large scale effective string, this anomaly is known to disappear at large distances [12], which is the region we are interested in.

Inserting this result in eq.(14) and setting for simplicity $d = 3$ (i.e. only one transverse degree of freedom)⁶ we end up with

$$S[X] = \sigma \int_0^L dx_1 \int_0^R dx_2 \sqrt{1 + (\partial_\tau X)^2 + (\partial_\varsigma X)^2} . \quad (19)$$

⁶With this choice the quartic terms in eq.(18) cancel out and the expression simplifies. Notice that if one is interested in the action for $d > 3$ these terms survive. This is the reason for which in the final result one finds a non-trivial dependence on d . A nice way to understand this fact is to notice that the self-interaction of the string also couples different transverse degrees of freedom.

Let us now expand the square root. As a first step, in order to correctly identify the expansion parameter let us rewrite the action in terms of adimensional variables. Let us define: $\phi = \sqrt{\sigma}X$, $\xi_1 = \tau/R$, $\xi_2 = \varsigma/L$. In this way we recognize that the expansion parameter is $(\sigma LR)^{-1}$. Expanding the action keeping only the first two orders (i.e. keeping only terms up to the fourth order in the fields) we find:

$$S[X] = \sigma LR + S'(\phi) \ , \quad (20)$$

where

$$S'(\phi) = S_G(\phi) - \frac{1}{8\sigma LR} S_p(\phi) + O\left((\sigma LR)^{-2}\right) \ . \quad (21)$$

Let us look at these two terms in more detail:

- S_G is a purely Gaussian term

$$S_G(\phi) = \frac{1}{2} \int_0^1 d\xi_1 \int_0^1 d\xi_2 (\nabla\phi)^2 \quad (22)$$

with

$$(\nabla\phi)^2 = \frac{1}{2u} \left(\frac{\partial\phi}{\partial\xi_1} \right)^2 + 2u \left(\frac{\partial\phi}{\partial\xi_2} \right)^2 \quad (23)$$

and

$$u = \frac{L}{2R} \ . \quad (24)$$

It is easy to see that this term is exactly the free field action discussed in sect. 2.4. At this level of approximation the partition function becomes

$$Z(L, R) = \exp(-\sigma LR) Z_1 \ , \quad (25)$$

where Z_1 is the Gaussian integral evaluated in sect. 2.4

$$Z_1 = \frac{1}{\eta(iu)} \ . \quad (26)$$

It is easy to see that this result holds also for $d > 3$, each transverse degree of freedom being independent from the other so that the final result is simply the product of $(d - 2)$ times the Dedekind function. Thus we exactly recover the result of eq.(10).

- S_p is the “self-interaction term”:

$$S_p(\phi) = \int_0^1 d\xi_1 \int_0^1 d\xi_2 \left[(\nabla \phi)^2 \right]^2 . \quad (27)$$

At order $(\sigma LR)^{-1}$ the partition function is therefore

$$Z(L, R) = \exp(-\sigma LR) Z_1 \left(1 + \frac{1}{8\sigma LR} \langle S_p \rangle \right) , \quad (28)$$

where the expectation value of S_p is taken with respect to the action S_G . Also this expectation value can be evaluated using the ζ -function regularization. The calculation can be found in [22]:

$$\langle S_p \rangle = \frac{\pi^2}{36} u^2 \left[2E_4(iu) - E_2^2(iu) \right] , \quad (29)$$

where E_2 and E_4 are the Eisenstein functions. The latter can be expressed in power series:

$$E_2(\tau) = 1 - 24 \sum_{n=1}^{\infty} \sigma(n) q^n \quad (30)$$

$$E_4(\tau) = 1 + 240 \sum_{n=1}^{\infty} \sigma_3(n) q^n \quad (31)$$

$$q \equiv e^{2\pi i \tau} , \quad (32)$$

where $\sigma(n)$ and $\sigma_3(n)$ are, respectively, the sum of all divisors of n (including 1 and n), and the sum of their cubes.

Bringing together the two terms we finally find (recall that we have fixed $d = 3$):

$$F_q^{(NLO)}(R, L) = \left[\log \eta(\tau) - \frac{\pi^2 L}{1152 \sigma R^3} \left[2E_4(\tau) - E_2^2(\tau) \right] \right] + O\left(\frac{1}{(\sigma LR)^2} \right) . \quad (33)$$

This is the functional form of the finite size corrections which we shall compare with the results of our Montecarlo simulations in sect. 4. Notice that the inclusion of next-to-leading terms does not require the introduction of any new free parameter, so that the predictive power is the same as for the free string case.

2.6 Implications for the deconfinement transition

One of the most interesting consequences of eq.s (8,13) is that in the large R limit the quantum fluctuations of the flux tube are proportional to R and have the effect to decrease the string tension. This change is proportional to T^2 and introduce a dependence on the finite temperature of the effective string tension:

$$\sigma(T) = \sigma(0) - \frac{\pi T^2(d-2)}{6} , \quad (34)$$

where $T = 1/L$ denotes the finite temperature and $\sigma(0)$ is the zero temperature limit of the string tension (which is measured, for instance, through Wilson loop expectation values). This process eventually leads to the deconfinement transition and can be used (see [26, 27]) to estimate the adimensional ratio $\sigma(0)/T_c^2$. If we assume that the free string picture holds for all temperatures up to T_c , eq.(34) would predict the value of the latter to be $T_c = \sqrt{6\sigma_0/\pi}$, a prediction that turns out to be rather far from the value obtained in Montecarlo simulations.

This is another reason which supports the existence of higher order terms in the effective string action. We can easily extend eq.(34) so as to keep into account the next to leading order in the Nambu-Goto action expansion. To this end, the modular transformation properties of the Eisenstein functions

$$E_2(\tau) = -\left(\frac{i}{\tau}\right)^2 E_2\left(-\frac{1}{\tau}\right) + \frac{6i}{\pi\tau} \quad (35)$$

$$E_4(\tau) = \left(\frac{i}{\tau}\right)^4 E_4\left(-\frac{1}{\tau}\right) \quad (36)$$

turn out to be very useful.

Performing a modular transformation so as to reach the large R limit we find

$$\begin{aligned} E_2\left(i\frac{L}{2R}\right) &= -\frac{4R^2}{L^2} E_2\left(i\frac{2R}{L}\right) + \frac{12R}{\pi L} \sim -\frac{4R^2}{L^2} \\ E_4\left(i\frac{L}{2R}\right) &= \frac{16R^4}{L^4} E_4\left(i\frac{2R}{L}\right) \sim \frac{16R^4}{L^4} \end{aligned} \quad (37)$$

so that

$$-\frac{1}{8\sigma LR} \langle S_p \rangle \sim -\frac{\pi^2 R}{72\sigma L^3} \quad (38)$$

and finally

$$F(L, R) \sim \sigma LR \left(1 - \frac{\pi}{6L^2\sigma} - \frac{\pi^2}{72\sigma^2 L^4} \right) . \quad (39)$$

This result perfectly agrees with the conjecture reported in [27, 26] which states that if the world sheet bordered by the two Polyakov loops is described by a Nambu-Goto type action then the string tension should vanish at the critical point with a square root singularity: $\sigma(T) \sim (T_c - T)^{\frac{1}{2}}$. This behavior is compatible with eq.(34) only if we assume:

$$\sigma(T) = \sigma(0) \sqrt{1 - \frac{T^2}{T_c^2}} \quad (40)$$

with

$$T_c^2 = \frac{3\sigma(0)}{\pi} , \quad (41)$$

which turns out to be in much better agreement with the results of MC simulations.

Inserting this value into eq.(39) we find:

$$F(L, R) \sim \sigma \frac{R}{T} \left(1 - \frac{1}{2} \left(\frac{T}{T_c} \right)^2 - \frac{1}{8} \left(\frac{T}{T_c} \right)^4 \right) \quad (42)$$

which is exactly the expansion to the next to leading order of eq.(40).

Even if the estimate of eq. (41) predicts a value for the ratio $T_c^2/\sigma(0)$ which is in good agreement with the existing Montecarlo estimates for SU(N) LGTs, it should be considered with great caution, since it predicts a critical index 1/2 for the deconfinement transition which disagrees both with Montecarlo results and with the expectations of the Svetitsky-Yaffe conjecture. This means that assuming a Nambu-Goto type action is probably too naive and/or that the regularization of higher perturbative orders introduces new terms in the large R limit.

However, notwithstanding this cautionary observation, the previous discussion certainly tells us that the simple free bosonic theory cannot be the end of the story and that higher order terms must necessarily be present to match with the expected behavior near the deconfinement transition.

2.7 Range of validity of the effective string picture

As mentioned in the previous sections, the effective string picture is expected to hold at large enough distances (see in particular the comments in sect. 2.2). However one of the surprising features of the recent Montecarlo results [18, 9] is that the effective string picture seems indeed to hold at remarkably small distances. In [18] (Wilson loop operators in $d = 4$ SU(3) LGT) the range of validity starts at $R_c \sim 0.4$ fm. (In the following we shall denote with R_c the minimum value of interquark distance at which we expect the effective string picture, possibly with higher order corrections, to hold). A similar result is also reported in [9] (Polyakov loop correlators in $d = 3$ and $d = 4$ SU(3) LGT), with $0.4 \lesssim R_c \lesssim 0.5$ fm.

As for the Ising model, we found looking at the Wilson loop expectation values that [5] $\sigma R_c^2 \sim 1.5$ (see fig. 2 of ref. [5]). In exactly the same range of values also the logarithmic increase of the flux tube starts to hold, in agreement with the effective string predictions (see the comment at page 408 of [14]). If (with abuse of language) we try to write these scales in fermi units using the definition of the Sommer scale r_0 which is given by $\sigma r_0^2 = 1.65$, we see that also in the Ising case we find $0.4 \lesssim R_c \lesssim 0.5$ fm. Following [5] we shall assume that also in our present analysis $R_c = \sqrt{\frac{1.5}{\sigma}}$.⁷

All these observations show that the scale R_c is much smaller than what one would naively expect and that it seems to show a remarkable degree of universality. It would be very interesting to understand the reason of this behavior.

When dealing with Polyakov loop correlators, a natural scale to measure distances is the critical temperature T_c , which is related to the string tension by [29]

$$\frac{T_c}{\sqrt{\sigma}} = 1.2216(24) \quad . \quad (43)$$

For $L_c = 1/T_c$ we hence get $\sigma L_c^2 \sim 0.67$. This implies that $L_c \sim 0.3$ fm and $R_c \sim 1.5 L_c$.

⁷The presence of this threshold of validity is the main reason why earlier studies in the 3d Ising gauge model, probing shorter physical distances, due to the smaller computational power available, could not identify the free bosonic string as the correct model and actually suggested a fermionic string model [28]. It is now clear that, at least in the range of values that we studied in the present paper, such a picture is not supported by the data.

In view of the above discussion it is useless to look at correlators below the scale L_c , since in that region the string picture certainly does not hold. At the same time it is interesting to explore the scales below R_c in the range $L_c < R < R_c$ to see if the value of R_c is again confirmed and/or if higher order effects can in part take into account the deviation from the free string picture below R_c .

3 Simulations

3.1 3d gauge Ising model

In order to test our predictions we performed a set of simulations on the 3d \mathbb{Z}_2 gauge model, whose partition function can be obtained from the general expression in eq. (1) by setting $U_l \equiv \sigma_l \in \{1, -1\}$. The resulting partition function turns out to be

$$Z_{gauge}(\beta) = \sum_{\{\sigma_l = \pm 1\}} \exp(-\beta S_{gauge}) . \quad (44)$$

The action S_{gauge} is a sum over all the plaquettes of a cubic lattice,

$$S_{gauge} = - \sum_{\square} \sigma_{\square} \quad , \quad \sigma_{\square} = \sigma_{l_1} \sigma_{l_2} \sigma_{l_3} \sigma_{l_4} . \quad (45)$$

As in eq. (1), we choose the same coupling in the time-like and in the two space-like directions of the cubic lattice.

This model is known to have a roughening transition at $\beta_r = 0.47542(1)$ [30], and a bulk (i.e. at zero temperature) deconfinement transition at $\beta_c = 0.7614133(22)$ [31]. We performed our Montecarlo simulations at three different values of the coupling constant β , all located in the rough phase and close enough to the deconfinement point to be well within the scaling region. We chose three values for which the deconfinement temperature (and hence the critical distance R_c) was known with high precision so as to be able to precisely fix the minimal distance between the Polyakov loops and the lattice size in the time direction.

It is important to recall that the 3d gauge Ising model can be translated into the 3d spin Ising model by the so called Kramers-Wannier duality

transformation

$$Z_{gauge}(\beta) \propto Z_{spin}(\tilde{\beta}) \quad (46)$$

$$\tilde{\beta} = -\frac{1}{2} \log [\tanh(\beta)] \quad , \quad (47)$$

where Z_{spin} is the partition function of the Ising model in the dual lattice:

$$Z_{spin}(\tilde{\beta}) = \sum_{s_i = \pm 1} \exp(-\tilde{\beta} H_1(s)) \quad (48)$$

with

$$H_1(s) = - \sum_{\langle ij \rangle} J_{\langle ij \rangle} s_i s_j \quad , \quad (49)$$

where the sum runs over the links $\langle ij \rangle$ connecting the nearest-neighbor sites i and j . Here the couplings $J_{\langle ij \rangle}$ are fixed to the value $+1$ for all the links. This relation defines a one-to-one mapping between the free energy densities in the thermodynamic limit.

The expectation values of gauge invariant observables can be expressed as ratios of partition functions of the spin model. For instance the dual of the Polyakov loop correlators, in which we are presently interested, is given by

$$\langle P(x) P^\dagger(x + R) \rangle = \frac{Z_{spin,S}(\tilde{\beta})}{Z_{spin}(\tilde{\beta})} \quad , \quad (50)$$

where in $Z_{spin,S}$ all the couplings of the links (in the dual lattice) that intersect a surface S joining the two loops (any choice of the surface joining the two loops is equivalent) take the value $J_{\langle ij \rangle} = -1$. This construction explains why the results that we are discussing are related (apart from the different choice of boundary conditions) to those obtained studying the interfaces of the 3d Ising spin model.

For the ratios of correlators that we shall study below, we get

$$\frac{G(R)}{G(R+1)} = \frac{Z_{spin,L \times R}(\tilde{\beta})}{Z_{spin,L \times (R+1)}(\tilde{\beta})} \quad , \quad (51)$$

where we have taken the minimal surfaces that join the Polyakov loops. Eq. (51) is the basis of the algorithm that we shall discuss below.

3.2 The algorithm

Computing the Polyakov-loop correlation function in the lattice gauge theory in the straight forward way, the statistical error is increasing exponentially with L and R . On the other hand the value of $G(R)$ is decreasing exponentially with R . This problem is partially resolved by the algorithm of Lüscher and Weisz [8].

Our approach in the dual model overcomes the problem completely. The statistical error of the ratio $G(R)/G(R+1)$ virtually does not depend on L and R . The numerical results show that already for $R = 2$ our method in the dual model gives similar statistical errors as the direct measurement in the gauge model. For instance, in the $\beta = 0.73107$ case, with $L = N_t = 8$ we find with the present algorithm $G(5)/G(4) = 0.68421(9)$ (see tab. 3) to be compared with the value $G(5)/G(4) = 0.68429(21)$ obtained with the direct measurement and used in our previous paper [7].

Our method is essentially an improved version of the so called “snake algorithm” introduced in [32] to study the ’t Hooft loop in $SU(2)$ LGT’s and later adapted to the study of the interface free energy in the 3d spin Ising model [33]. The major improvement in our algorithm with respect to ref.s [32, 33] is the hierarchical organization of the lattice updates (see below) which allows us to greatly enhance the precision of our results. Let us see in detail our algorithm.

In order to compute eq. (51) numerically, we factorize the ratio of partition functions in such a way that for each factor the partition functions differ just by the value of $J_{\langle ij \rangle}$ at a single link

$$\frac{Z_{L \times R}}{Z_{L \times (R+1)}} = \frac{Z_{L \times R, 0}}{Z_{L \times R, 1}} \cdots \frac{Z_{L \times R, M}}{Z_{L \times R, M+1}} \cdots \frac{Z_{L \times R, L-1}}{Z_{L \times R, L}}, \quad (52)$$

where we have suppressed the index *spin* and the argument $\tilde{\beta}$ to simplify the notation. $L \times R, M$ denotes a surface that consists of a $L \times R$ rectangle with a $M \times 1$ column attached. A sketch is given in fig. 1.

Each of the factors of eq. (52) can be written as expectation value in one of the two ensembles:

$$\frac{Z_{L \times R, M+1}}{Z_{L \times R, M}} = \frac{\sum_{s_i = \pm 1} \exp(-\tilde{\beta} H_{L \times R, M}(s)) \exp(-2\tilde{\beta} s_k s_l)}{Z_{L \times R, M}}, \quad (53)$$

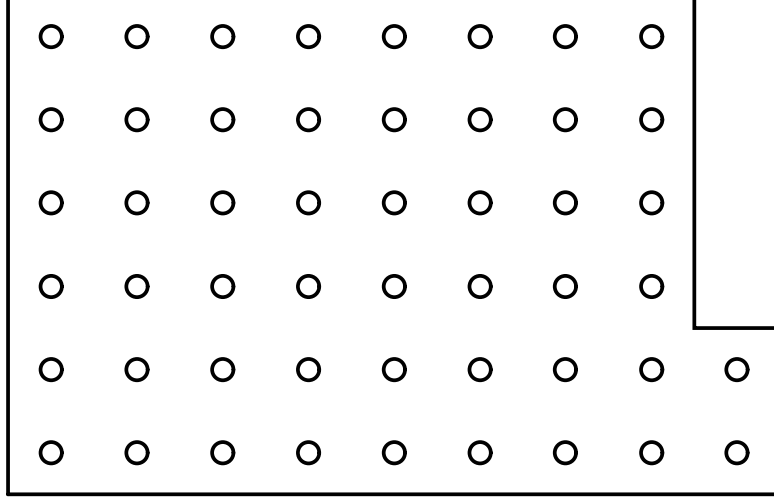


Figure 1: Sketch of the surface denoted by $L \times R, M$. In the example, $L = 6$, $R = 8$ and $M = 2$. The circles indicate the links that intersect the surface.

where $\langle k, l \rangle$ is the link that is added going from $L \times R, M$ to $L \times R, M + 1$. Note that already the ratio of partition functions in eq. (51) could be written as an expectation value in the ensemble for the $L \times R$ surface. However the corresponding observable has an enormous variance.

The observable that we measure has only support on a single link on the lattice. Therefore it would be quite a waste of time to update the whole lattice before measuring $s_k s_l$. In order to circumvent this problem we have enclosed the link $\langle kl \rangle$ in a sequence of sub-lattices of the size $b_{1,i} \times b_{2,i} \times b_{3,i}$. The center of each of the sub-lattices is the link $\langle kl \rangle$ and $b_{1,i} \leq b_{1,i+1}$, $b_{2,i} \leq b_{2,i+1}$ and $b_{3,i} \leq b_{3,i+1}$. i is running from 1 to n . In our simulation we have taken $n = 5$ throughout.

Now we perform update sweeps over these boxes in a hierarchical way. This can be best explained by the following piece of pseudo-code:

```
for(j_l=0; j_l<m_l; j_l++)
{
  for(k_l=0; k_l<t_l; k_l++) sweep over the whole lattice;
  for(j_n=0; j_n<m_n; j_n++)
```

```

{
for(k_n=0;k_n<t_n;k_n++) sweep over the sub-lattice n;
for(j_nm1=0;j_nm1<m_nm1;j_nm1++)
{
for(k_nm1=0;k_nm1<t_nm1;k_nm1++) sweep over the sub-lattice n-1;
.
.
.
for(j_1=0;j_1<m_1;j_1++)
{
for(i_1=0;i_1<t_1) sweep over the sub-lattice 1;
measure s_k s_l;
}
.
.
.
}
}
}

```

As basic update algorithm we have used the microcanonical demon-update with multi-spin coding implementation combined with a canonical update of the demon [34]. Details on the implementation can be found in refs. [35, 6]. In our implementation of multi-spin coding 32 or 64 lattices are simulated in parallel, depending on the architecture of the machine the program is running on. (Here we used Pentium 4 and Pentium III PC's; i.e. 32-bit machines. Hence 32 lattices are simulated in parallel).

In our simulations we have chosen the parameters of the algorithm ad hoc, without any attempt to optimize them. In particular we have always chosen 5 sub-lattices of increasing size and $m_1 = m_2 = \dots = m_5 = 10$. As an example, for $L = 24$ we have chosen sub-lattice sizes of $2 \times 3 \times 3$, $4 \times 5 \times 5$, $8 \times 9 \times 9$, $16 \times 17 \times 24$ and $32 \times 33 \times 24$. Note that the largest sub-lattices already take the full extent of the lattice in time direction.

In one cycle we performed $t_l = 5$ for $\tilde{\beta} = 0.228818$ and $\tilde{\beta} = 0.236025$ and $t_l = 10$ for $\tilde{\beta} = 0.226102$ complete sweeps over the lattice. In one instance we did sweep $t_1 = t_2 = \dots = t_5 = 2$ times over the sub-lattice. In our production runs, we always performed $m_l = 1000$ complete cycles.

That means that the total number of measurements for one value of M is $32 \times 1000 \times 10^5 = 3.2 \times 10^9$. Since $\exp(-\tilde{\beta}s_k s_l)$ can take only two values, the expectation value of $\exp(-\tilde{\beta}s_k s_l)$ can be easily obtained from the expectation value of $s_k s_l$. Therefore, in the program, we accumulated $s_k s_l$ rather than $\exp(-\tilde{\beta}s_k s_l)$ itself. Averages of $s_k s_l$ over whole cycles were written to a file for later analysis.

Before we started the measurement, 8000 sweeps over the whole lattice were performed for $\tilde{\beta} = 0.228818$ and $\tilde{\beta} = 0.236025$ and 16000 sweeps for $\tilde{\beta} = 0.226102$ for equilibration.

In order to get a good estimate of autocorrelation times we performed one more extended run for $\tilde{\beta} = 0.226102$, $L = 24$, $R = 24$ and $M = 0$ with 10000 complete cycles. For the cycle averages of $s_k s_l$ we obtain $\tau_{int} = 0.92(5)$ in units of cycles. To deal with the large number of simulations, the analysis had to be automated. Computing the statistical error, we performed a binning analysis with 50 bins i.e. a bin size of 20 throughout. Given the small autocorrelation time, this bin size should be sufficient.

As an example, we give the individual results for $Z_{L \times R, M+1}/Z_{L \times R, M}$ for $\tilde{\beta} = 0.226102$, $L = 24$ and $R = 24$ in table 1. Classically, one expects $Z_{L \times R, M}/Z_{L \times R, M+1} = \exp(-\sigma) = \exp(-0.010560) = 0.9895\dots$. In fact, the results for $1 < M < 22$ are rather close to this value. Note that $Z_{L \times R, 0}/Z_{L \times R, 1}$ is much smaller and $Z_{L \times R, L-1}/Z_{L \times R, L}$ much larger than this value. I.e. it is unfavorable to create corners and favorable to eliminate them.

The statistical error of $Z_{L \times R+1}/Z_{L \times R}$ in table 1 is on average a little less than 0.00003. Given the expectation value, it is easy to compute the variance of $\exp(-2\tilde{\beta}s_k s_l)$, since it can assume only the value $\exp(2\tilde{\beta})$ or $\exp(-2\tilde{\beta})$. Let us denote the probability for the two signs by p_+ and p_- . Then

$$p_+ + p_- = 1 \quad (54)$$

and

$$p_+ \exp(+2\tilde{\beta}) + p_- \exp(-2\tilde{\beta}) = \langle \exp(-2\tilde{\beta}s_k s_l) \rangle \approx 1 \quad (55)$$

Hence

$$p_+ \approx \frac{1 - \exp(-2\tilde{\beta})}{\exp(+2\tilde{\beta}) - \exp(-2\tilde{\beta})} \quad (56)$$

The variance of $\exp(-2\tilde{\beta}s_k s_l)$ is hence given by

$$\text{var}[\exp(-2\tilde{\beta}s_k s_l)] \approx p_+ \exp(+4\tilde{\beta}) + p_- \exp(-4\tilde{\beta}) - 1 \quad (57)$$

For $\tilde{\beta} = 0.226102$ we get $\text{var}[\exp(-2\tilde{\beta}s_k s_l)] \approx 0.208$. With this value for the variance, the statistical error of 0.00003 corresponds to $N_{eff} \approx 2.3 \times 10^8$ effectively independent measurements, which does not compare to bad with the 3.2×10^9 measurements that actually have been performed.

Note that the results for the individual values of M are obtained from completely independent simulations, i.e. computing the statistical error of $Z_{L \times R}/Z_{L \times (R+1)}$ we can use standard error-propagation. This becomes very simple, when we take the logarithm

$$\log\left(\frac{Z_{L \times R}}{Z_{L \times (R+1)}}\right) = \sum_{M=0}^{L-1} \log\left(\frac{Z_{L \times R, M}}{Z_{L \times R, M+1}}\right) . \quad (58)$$

Finally let us discuss the CPU-time that was needed for the simulations. E.g. for the $128 \times 128 \times 24$ lattice at $\tilde{\beta} = 0.226102$ the measurement for a single value of M takes about 125 min on a P4 1.7 GHz PC. The time for equilibration is about 17 min. I.e. the total time to compute $G(R+1)/G(R)$ is $24 \times (125 + 17) \text{ min} = 2 \text{ days and } 8 \text{ hours}$.

3.3 The simulation setting

We performed our simulations at three different values of β and various choices of N_t , N_s and R . In choosing these values we had to face four major constraints:

- a] The lattice size in the space-like directions N_s must be large enough so as to avoid unwanted finite size effects due to the rather large values of the correlation lengths that we shall study. Experience with the model suggests that any value $N_s \geq 10\xi$ should solve this problem (see for instance [36]).
- b] The distance R between the two Polyakov loops should be larger than the inverse of the critical temperature (see the discussion in sect. 2.7) i.e. $R \geq L_c(\beta) = N_{t,c}(\beta)$.
- c] The values of β that we choose must be in the scaling region. This is needed at least for two reasons. The first (and obvious) one is that we do not want to mix the finite size effects that we plan to observe (which are expected to be very small) with unwanted effects due to

scaling violations. The second reason is that, as we shall discuss below, we need a very precise estimate of the zero temperature string tension in order to perform our analysis. This requires a careful extrapolation of the known values of the string tension to the values of β at which we perform our simulations. Therefore high precision results for the string tension for a rather dense set of β -values should be available in the literature. Taking refs. [37, 6, 38], this means that we should have $\beta > 0.73$.

- d] We want to study the range of T in which the precise functional form of the string corrections is most important. This means that we should explore the region $T_c > T > T_c/3$.

From the above discussion we see that a central role is played by the value of $N_{t,c}$, so we decided to choose three values of β for which the critical temperature was known with high precision. The natural choice was $\beta = 0.73107$ for which $N_{t,c} = 4$; $\beta = 0.746035$ to which corresponds $N_{t,c} = 6$ and finally $\beta = 0.75180$ for which $N_{t,c} = 8$ (these values are taken from [29]). This choice fulfills constraint [c]. Further details on the parameters of the simulations can be found in tab. 2 where we also list for completeness the values of the correlation length and the zero temperature string tension for these three values of β . Since the precise value of $\sigma(0, \beta)$ at the three values of β that we studied will play an important role in the following, it is worthwhile to shortly discuss how we extracted these estimates from the literature. The first important observation is that, due to the high precision of our data and to the relative distance from the critical point we cannot simply rely on the asymptotic scaling estimate of $\sigma(0)$. A much better (and precise enough for our purpose) estimate can be obtained taking as reference values those published in [37, 6, 38]⁸ and then interpolating among them with the law

$$\sigma(0, \beta) = \sigma(0, \beta_{ref}) \left(\frac{\beta - \beta_c}{\beta_{ref} - \beta_c} \right)^{2\nu}, \quad (59)$$

where β_{ref} is the coupling at which the reference value of σ is taken and β_c is the critical temperature. If $|\beta - \beta_{ref}|$ is small enough, both the uncertainty in

⁸We also used some unpublished values of σ obtained as a byproduct of the work published in [38].

ν and the systematic error due to neglecting higher order terms in the scaling law can be neglected. The systematic error induced by this approximation can be estimated by repeating the same analysis with another nearby value of β_{ref} . The difference between the two results for $\sigma(0, \beta)$ obtained in this way gives a good estimate of this systematic error. The final error on σ is the sum of the above systematic error plus the statistical errors of $\sigma(0, \beta_{ref})$ (as quoted in ref.s [37, 6, 38]).

Besides the simulations with the choice of parameters reported in tab. 2 we also studied, in order to have a cross-check of our finite size effect predictions, (only in the case of $\beta = 0.74603$) several values of N_t keeping R fixed at the value $R = 24$ (notice that for this value of β we have $R_c \sim 9$ so with $R = 24$ we are deep in the region of validity of the effective string picture). The results are reported in tab. 6.

4 Discussion of the results

For all the values of β and N_t listed in tab. 1 we extracted from the simulations the expectation values of the ratios

$$\frac{G(R+1)}{G(R)} \equiv \frac{\langle P(x)P^\dagger(x+R+1) \rangle}{\langle P(x)P^\dagger(x+R) \rangle} . \quad (60)$$

We studied only a selected sample of values of R . The results of the simulations are reported in tabs 3,4 and 5. Notice that, since each value of R corresponds to a different simulation all values reported in tabs 3, 4 and 5 are completely uncorrelated.

From these ratios we constructed the quantity:

$$Q_0(R) = \log \left(\frac{G(R)}{G(R+1)} \right) . \quad (61)$$

If no string effect is present the correlator should follow the pure strong coupling behavior of eq.(4). Then it is easy to see that we should have

$$Q_{0,cl} = \sigma L . \quad (62)$$

So, in order to select the finite size corrections in which we are interested we defined:

$$Q_1(R) = \log \left(\frac{G(R)}{G(R+1)} \right) - \sigma L . \quad (63)$$

We plot in fig.s 2-5 our data together with the prediction for Q_1 of the pure string contribution (the simple Dedekind function) and the Nambu-Goto correction eq.(33) for the four values of N_t at $\beta = 0.75180$. For each value of N_t we report in the figure caption the value of $z_c \equiv \frac{2R_c}{N_t}$ beyond which the effective string picture is expected to hold (see the discussion in sect. 2.7). The data for the other two values of β show a similar behavior as it can be easily checked using the values reported in tab.s 3,4 and 5.

$Q_1(R)$ is affected by two different types of uncertainties. The one due to the Polyakov loop correlators and that due to σ (let us call it $\delta\sigma$). The two must be treated differently. We encoded the statistical errors of the Polyakov correlators as usual with the error bars, while we kept into account the uncertainty in σ by plotting in the figures (both for the Nambu Goto corrections and for the pure string term) two curves obtained using $\sigma + \delta\sigma$ and $\sigma - \delta\sigma$, respectively.

In fig. 6 we plot the data at fixed R reported in tab. 6.

Few comments are in order.

- a] Finite size corrections with respect to the pure classical law of eq.(4) are certainly present in the Polyakov loop correlators. In fact the deviation from the pure area law expectation (which is $Q_1 = 0$) is immediately evident from the figures.
- b] For the lowest temperature that we studied, i.e. $T = T_c/3$, the contribution of the first correction of the Nambu-Goto string is almost of the same order of magnitude of the uncertainty in the string tension (see fig. 2). This is the reason why we chose to study higher values of T/T_c ⁹.
- c] As the temperature increases, the gap between the pure bosonic string prediction and the Nambu-Goto one becomes larger and larger. It is clear, looking at the figures, that the pure bosonic string (continuous lines in fig.s 2-6) does not describe the data in this temperature range. The disagreement is most probably the signature of the fact that effective string underlying the 3d gauge Ising model is actually a self-interacting string. It is easy to guess that the contribution due to this

⁹Notice however that for very low values of T/T_c (like those studied in [9]) the contribution due to the first order correction to the Nambu-Goto string increases again in magnitude (but has the opposite sign) in the small R region (but has the opposite sign).

self-interaction becomes more and more important as the temperature increases, and this is indeed confirmed by the data. The data suggest that the main effect of this self-interaction is to lower the value of the string tension. As discussed in sect. 2.6, this effect is already present with the simple free bosonic string, but the lowering is enhanced by the self-interaction.

- d] There is a remarkable agreement between the data and the functional form of eq.(33) which describes the first correction of the Nambu-Goto string with respect to the free bosonic string. It is important to stress that this agreement is not the result of a fitting procedure. There is no free parameter in eq. (33).
- e] The agreement becomes worse and worse as R decreases. The deviations are particularly evident in the $R < R_c$ region ($z < z_c$ in fig.s 2-5). This could be simply due to the fact that one is approaching the size of the flux tube thickness, but could also indicate that the functional form that we use is inadequate in the small z region, or that a smooth cross-over is present toward a different string picture.
- f] The data show a very good scaling behavior: once the proper value of $\sigma(\beta)$ is subtracted, no further dependence on β is present (this is the reason why we needed very precise independent estimates for $\sigma(\beta)$)
- g] The agreement is particularly impressive for the last set of data, i.e. those taken at fixed $R = 24$ and shown in fig. 6. In this case, for $N_t > 12$ the prediction of eq.(33) agrees with the data within the errors (which, thanks to the nature of our algorithm, are very small even if R is large). It is worthwhile to notice that for this value of β we have $R_c \sim 9$.

In the definition of Q_1 we must insert the exact value of the string tension. In principle it would be nice to avoid this external parameter and construct a combination of Polyakov loop correlators in which only the effective string corrections appear, without additional terms. This is easily achieved by the combination

$$H(R, k) \equiv Q_1(R - k) - Q_1(R) \quad (64)$$

which is similar (apart from a different normalization) to the function $c(r)$ discussed in [9]. However it is easy to see, looking at the large R expansions

of eq.(13) and (37) that this is not a good choice in the large z region that we study here, where the contributions to $H(R)$ from the pure bosonic string and from the Nambu Goto correction decrease as $1/R^2$ and $1/R^3$ respectively. On the contrary $H(R, k)$ turns out to be a very useful quantity in the small z region (as in the case of [9]). This is well exemplified by fig. 7, where we plotted $H(R, 1)$ as a function of z for an hypothetical set of data with $L = 60$ and R ranging from 6 to 30 (i.e. $z < 1$). In fig. 8 we report $H(R, 2)$ for our data at $\beta = 0.74603$ and $L = 12$. The data agree with the Nambu-Goto prediction, but the errors (even if very small) are of the same order of magnitude of the difference between the pure bosonic string and the Nambu-Goto correction. This is just another way to say that the major contribution of effective string fluctuations to the interquark potential in the large z limit is simply a temperature dependence of the string tension and it is exactly this signature that we observe looking at the Q_1 observable.

5 Conclusions

Despite the impressive agreement which is manifest in fig.s 2-6, our analysis leaves several open problems.

- 1] If we really assume that the Nambu-Goto proposal is the correct description for the effective string, then the agreement that we find becomes rather embarrassing, since there is apparently no room left for the higher order corrections which one should expect in this framework. In principle one could guess that these higher order correction are negligible, but this can be hardly reconciled with the expected large R behavior. For R large enough, the only term which survives is the finite renormalization of the string tension which for the Nambu-Goto string is expected [26] to be simply given, order by order, by the expansion of the square root in eq.(40), and these terms are certainly not negligible.

This observation agrees with the results recently appeared in [39] where the spectrum of string excitation in the $d = 4$ $SU(3)$ LGT was studied. The observed spectrum seems to disagree both with the predictions of the pure bosonic string and with that of the Nambu-Goto model. It

would be interesting to study the same spectrum directly in the 3d gauge Ising model.

- 2] Comparing our results with what Lüscher and Weisz find in the $d=3$ and 4 $SU(3)$ LGT [9] we see that the three models seem to be described by three different effective string theories, with the same large distance limit (the free bosonic string) but different self-interaction terms. In fact in the $d=3$ case they find a perfect agreement with the pure free string contribution and higher order self-interaction terms seem to be absent. In $d=4$ they find higher order corrections which are modeled by a boundary-type term. We checked that these deviations from the free string behavior do not agree with the $d = 4$ version of the Nambu Goto correction of eq. (33). In principle there is no reason to expect the same effective string in the 3d gauge Ising model and in the 3d and 4d $SU(3)$ ones, however in past years it has become a common attitude to think that the effective string model underlying a given LGT only feels the geometry of the observables and is independent of the particular gauge group which one is studying. The present numerical results and those of [9] suggest that this is not the case and that we are in presence of a variety of different effective strings. In this respect it would be very interesting to have results from some other models in $d = 3$ so as to have a larger statistics and see if we are really dealing with different effective strings [40]. Notice, as a side remark, that we are looking to a different range of values of z with respect to [9]. In principle it is also possible that the two LGT's show the same behavior if they are studied in the same range of z values.
- 3] Several independent results (and in particular the experience with the dual problem of the interface fluctuations in the 3d Ising spin model) suggest that in the 3d gauge Ising model the parameter which controls the effective string fluctuations is the stiffness rather than the string tension. The two coincide at the critical point, share the same leading scaling behavior in the scaling region, but have different subleading corrections. Unfortunately there is presently no reliable estimate of the stiffness in the scaling region, thus we are unable to estimate the difference with respect to the string tension and evaluate the correction that it induces in our estimates. However, since we study three different

values of β , where this effect should be quite different in amplitude, we are confident that our qualitative results are not questioned by this problem.

Our results naturally raise the question whether the effective string underlying the Ising model is of the Nambu-Goto type or not. In view of the above discussion, we are not presently able to answer in a definite way. What we can state with confidence is:

- At large enough distances and low enough temperatures the data are well described by a simple free effective bosonic string theory. Besides the Ising models, the same seems to be true for SU(3) LGT in d=3 and d=4 [9, 18].
- At shorter distances and/or higher temperatures, the effective string picture still holds, but corrections due to boundary-type terms or to self-interaction terms in the string action appear. The Montecarlo simulations suggest that these corrections are different in the various models.
- The peculiar geometry of the Polyakov loop correlators (in particular the fact that the inverse temperature is related to the length of the Polyakov loops) implies that they are perfect tools to explore this region and detect higher order terms which must necessarily show up, even for large values of R , as the critical temperature is approached.
- At large distances these higher order terms act to lower the string tension, while at short distances they behave as $1/R^n$ corrections with $n > 1$.
- In the 3d gauge Ising model that we studied in this paper the data remarkably agree with the predictions of the Nambu-Goto action, truncated at the first perturbative order.

It is clear from this discussion that there is still a very long way before we can reach a precise understanding of the effective string underlying lattice gauge theory. However we are now in a much better position than before since new powerful numerical algorithms (one of them is described in this

paper) recently entered the game [8, 9]. The goal is worthwhile and certainly justifies further efforts in this direction.

Acknowledgements We are deeply indebted to P. Provero for many useful suggestions and discussions. We thank R. Sommer for a final reading of the draft. This work was partially supported by the European Commission TMR programme HPRN-CT-2002-00325 (EUCLID).

References

- [1] H. B. Nielsen and P. Olesen, “*Vortex Line Models For Dual Strings*”, Nucl. Phys. **B61** (1973) 45.
G. ’t Hooft, “*A Two-Dimensional Model For Mesons*”, Nucl. Phys. **B75** (1974) 461.
K. G. Wilson, “*Confinement Of Quarks*”, Phys. Rev. **D10** (1974) 2445.
A. M. Polyakov, “*String Representations And Hidden Symmetries For Gauge Fields*”, Phys. Lett. **B82** (1979) 247.
A. M. Polyakov, “*Gauge Fields As Rings Of Glue*”, Nucl. Phys. **B164** (1980) 171.
J. Gervais and A. Neveu, “*The Quantum Dual String Wave Functional In Yang-Mills Theories*”, Phys. Lett. **B80** (1979) 255.
Y. Nambu, “*QCD And The String Model*”, Phys. Lett. **B80** (1979) 372.
- [2] M. Lüscher, K. Symanzik and P. Weisz, “*Anomalies Of The Free Loop Wave Equation In The Wkb Approximation*”, Nucl. Phys. **B173** (1980) 365.
M. Lüscher, “*Symmetry Breaking Aspects Of The Roughening Transition In Gauge Theories*”, Nucl. Phys. **B180** (1981) 317.
- [3] A.A. Belavin, A.M. Polyakov and A.B. Zamolodchikov, “*Infinite Conformal Symmetry in two-dimensional Quantum Field Theory*”, Nucl. Phys. **B241** (1984) 333.
- [4] For a comprehensive review on CFT’s see for instance chapter 9 of:
C. Itzykson and J.-M. Drouffe, “*Statistical Field Theory*”, Cambridge 1989.
- [5] M. Caselle, R. Fiore, F. Gliozzi, M. Hasenbusch and P. Provero, “*String effects in the Wilson loop: A high precision numerical test*”, Nucl. Phys. **B486** (1997) 245 [arXiv:hep-lat/9609041].
- [6] M. Caselle, R. Fiore, F. Gliozzi, M. Hasenbusch, K. Pinn and S. Vinti, “*Rough interfaces beyond the Gaussian approximation*”, Nucl. Phys. B **432** (1994) 590 [arXiv:hep-lat/9407002].

- [7] M. Caselle, M. Panero and P. Provero, “*String effects in Polyakov loop correlators*”, JHEP **0206** (2002) 061 [arXiv:hep-lat/0205008].
- [8] M. Lüscher and P. Weisz, “*Locality and exponential error reduction in numerical lattice gauge theory*”, JHEP **0109** (2001) 010 [arXiv:hep-lat/0108014].
- [9] M. Lüscher and P. Weisz, “*Quark confinement and the bosonic string*”, arXiv:hep-lat/0207003.
- [10] A. Hasenfratz, E. Hasenfratz and P. Hasenfratz, “*Generalized Roughening Transition And Its Effect On The String Tension*”, Nucl. Phys. **B180** (1981) 353.
C. Itzykson, M. E. Peskin and J. B. Zuber, “*Roughening Of Wilson’s Surface*”, Phys. Lett. **B95** (1980) 259.
- [11] J. Greensite and C. B. Thorn, “*Gluon chain model of the confining force*”, JHEP **0202**, 014 (2002) [arXiv:hep-ph/0112326].
- [12] P. Olesen, “*Strings And QCD*”, Phys. Lett. **B160** (1985) 144.
- [13] M. Lüscher, G. Munster and P. Weisz, “*How Thick Are Chromoelectric Flux Tubes?*”, Nucl. Phys. **B180** (1981) 1.
- [14] M. Caselle, F. Gliozzi, U. Magnea and S. Vinti, “*Width of Long Colour Flux Tubes in Lattice Gauge Systems*”, Nucl. Phys. **B460** (1996) 397 [arXiv:hep-lat/9510019].
- [15] H. W. Bloete, J. L. Cardy and M. P. Nightingale, “*Conformal Invariance, The Central Charge, And Universal Finite Size Amplitudes At Criticality*”, Phys. Rev. Lett. **56** (1986) 742.
I. Affleck, “*Universal Term In The Free Energy At A Critical Point And The Conformal Anomaly*”, Phys. Rev. Lett. **56** (1986) 746.
- [16] C. Itzykson, H. Saleur and J.-B. Zuber, “*Conformal Invariance of Nonunitary Two-Dimensional Models*”, Europhys. Lett. **2** (1986) 91.
- [17] J.L. Cardy, “*Effect of Boundary Conditions on the Operator Content of Two-Dimensional Conformally Invariant Theories*”, Nucl. Phys. **B275**

- (1986) 200, “*Boundary Conditions, fusion Rules and the Verlinde Formula*”, Nucl. Phys. **B324** (1989) 581.
- [18] S. Necco and R. Sommer, “*The $N(f) = 0$ heavy quark potential from short to intermediate distances*” Nucl. Phys. B **622** (2002) 328 [arXiv:hep-lat/0108008].
 - [19] B. Lucini and M. Teper, “*Confining strings in $SU(N)$ gauge theories*”, Phys. Rev. D **64** (2001) 105019 [arXiv:hep-lat/0107007].
 - [20] F. Gliozzi and P. Provero, “*The confining string and its breaking in QCD*”, Nucl. Phys. B **556** (1999) 76 [arXiv:hep-lat/9903013].
 - [21] M. Minami, “*How ‘Can One Hear The Shape Of A Drum’ In The Dual Partition Functions?*”, Prog. Theor. Phys. **59** (1978) 1709.
 - [22] K. Dietz and T. Filk, “*On The Renormalization Of String Functionals*”, Phys. Rev. D **27** (1983) 2944.
 - [23] M. Flensburg and C. Peterson, “*String Model Potentials And Lattice Gauge Theories*”, Nucl. Phys. B **283** (1987) 141.
 - [24] P. de Forcrand, G. Schierholz, H. Schneider and M. Teper, “*The String And Its Tension In $SU(3)$ Lattice Gauge Theory: Towards Definitive Results*”, Phys. Lett. B **160** (1985) 137.
 - [25] P. Provero and S. Vinti, “*Capillary Wave Approach To Order-Order Fluid Interfaces In The 3-D Three State Potts Model*”, Physica A **211** (1994) 436 [arXiv:hep-lat/9310028].
 - [26] P. Olesen, “*Strings, Tachyons And Deconfinement*”, Phys. Lett. B **160** (1985) 408.
 - [27] R. D. Pisarski and O. Alvarez, “*Strings At Finite Temperature And Deconfinement*”, Phys. Rev. D **26** (1982) 3735.
 - [28] M. Caselle, R. Fiore, F. Gliozzi and S. Vinti, “*The Effective string of 3-D $Z(2)$ gauge theory as a $c = 1$ compactified CFT*”, Int. J. Mod. Phys. A **8** (1993) 2839 [arXiv:hep-lat/9207001].

- [29] M. Caselle and M. Hasenbusch, “*Deconfinement transition and dimensional cross-over in the 3D gauge Ising model*”, Nucl. Phys. B **470** (1996) 435 [arXiv:hep-lat/9511015].
- [30] M. Hasenbusch and K. Pinn, “*Computing the Roughening Transition of Ising and Solid-On-Solid Models by BCSOS Model Matching*”, J. Phys. A **30** (1997) 63 [arXiv:cond-mat/9605019].
- [31] H. W. Blöte, L. N. Shchur and A. L. Talapov, “*The Cluster Processor: New Results*”, Int. J. Mod. Phys. C **10** (1999) 1137-1148 [arXiv:cond-mat/9912005].
- [32] P. de Forcrand, M. D’Elia and M. Pepe, “*A study of the ’t Hooft loop in $SU(2)$ Yang-Mills theory*” Phys. Rev. Lett. **86** (2001) 1438 [arXiv:hep-lat/0007034].
P. de Forcrand, M. D’Elia and M. Pepe, “*The interaction between center monopoles in $SU(2)$ Yang-Mills*”, Nucl. Phys. Proc. Suppl. **94** (2001) 494 [arXiv:hep-lat/0010072].
- [33] M. Pepe and P. De Forcrand, “*Finite-size scaling of interface free energies in the 3d Ising model*” Nucl. Phys. Proc. Suppl. **106** (2002) 914 [arXiv:hep-lat/0110119].
- [34] K. Rummukainen, “*Multicanonical cluster algorithm and the 2-D seven state Potts model*”, Nucl. Phys. B **390** (1993) 621 [arXiv:hep-lat/9209024].
- [35] M. Hasenbusch and K. Pinn, “*Comparison of Montecarlo Results for the 3D Ising Interface Tension and Interface Energy with (Extrapolated) Series Expansions*”, Physica A **203** (1994) 189, [arXiv:hep-lat/9310013].
- [36] see for instance M. Caselle and M. Hasenbusch, “*Universal amplitude ratios in the 3D Ising model*,” J. Phys. A **A30** (1997) 4963 [arXiv:hep-lat/9701007].
- [37] M. Hasenbusch and K. Pinn, “*Surface tension, surface stiffness, and surface width of the three-dimensional Ising model on a cubic lattice*”, PhysicaA **192** (1993) 342 [arXiv:hep-lat/9209013].

- [38] M. Hasenbusch and K. Pinn, “*The interface tension of the 3D Ising model in the scaling region*” *Physica A* **245** (1997) 366 [arXiv:cond-mat/9704075].
- [39] K. J. Juge, J. Kuti and C. Morningstar, “*Fine structure of the QCD string spectrum*”, arXiv:hep-lat/0207004.
- [40] M.Caselle, M.Pepe and A.Rago, in preparation.

M	$Z_{L \times R, M+1}/Z_{L \times R, M}$
0	0.968311(25)
1	0.985483(29)
2	0.988214(23)
3	0.988921(23)
4	0.989258(29)
5	0.989387(24)
6	0.989479(22)
7	0.989538(28)
8	0.989590(25)
9	0.989560(24)
10	0.989665(26)
11	0.989660(27)
12	0.989720(27)
13	0.989742(30)
14	0.989750(28)
15	0.989775(28)
16	0.989780(26)
17	0.989866(26)
18	0.989988(32)
19	0.990072(29)
20	0.990396(29)
21	0.991146(23)
22	0.993860(26)
23	1.011208(30)

Table 1: As an example we give the results for the ratios of partition functions defined by eq. (53) $R = 24$, $L = 24$, $\tilde{\beta} = 0.226102$ on a $128 \times 128 \times 24$ lattice. The final result is $Z_{L \times (R+1)}/Z_{L \times R} = 0.77926(10)$.

β	$N_{t,c}$	N_t	N_s	ξ	σ	R_c
0.73107	4	6,8,12	64	1.41(3)	0.0440(3)	5.84
0.74603	6	9,12,18	96	2.09(4)	0.018943(32)	8.90
0.75180	8	10,12,16,24	128	2.95(10)	0.010560(18)	11.92

Table 2: A few information on our simulations. In the first column the value of β , in the second the inverse of the critical temperature. In the third and fourth columns the values of N_t and N_s that we studied. In the last three columns the values of the correlation length, the zero temperature string tension and the corresponding value of R_c .

R	$N_t = 6$	$N_t = 8$	$N_t = 12$
4	0.77558(11)	0.68421(9)	0.55275(10)
6	0.79682(14)	0.70519(10)	0.57304(11)
8	0.80850(14)	0.71627(10)	0.58320(13)
10	0.81628(15)	0.72351(11)	0.58943(14)
12	0.82151(18)	0.72825(12)	0.59387(16)
14	0.82540(20)	0.73183(14)	0.59692(18)
16	0.82798(20)	0.73487(15)	0.59956(19)
20	0.83215(21)	0.73870(16)	0.60266(20)
24	0.83564(25)	0.74134(17)	0.60522(22)
28	0.83769(30)	0.74332(21)	0.60734(24)

Table 3: Values of the ratio of two successive Polyakov loop correlators: $G(R+1)/G(R)$ for various values of R and N_t at $\beta = 0.73107$.

R	$N_t = 9$	$N_t = 12$	$N_t = 18$
6	0.84766(10)	0.78156(7)	
8	0.85912(11)	0.79336(8)	
10	0.86664(12)	0.80081(9)	
12	0.87219(13)	0.80607(9)	0.70586(7)
14	0.87586(14)	0.80992(11)	0.70955(8)
16	0.87908(15)	0.81310(11)	0.71235(8)
18	0.88145(17)	0.81539(13)	0.71464(9)
20	0.88356(17)	0.81731(13)	0.71611(9)
22	0.88468(17)	0.81906(13)	
24	0.88591(18)	0.82037(13)	0.71885(10)
26	0.88725(20)	0.82174(14)	
28	0.88854(20)	0.82249(15)	0.72086(11)
30	0.88941(20)	0.82354(16)	
32	0.89048(21)	0.82407(15)	0.72237(12)
36		0.82570(17)	
40		0.82691(18)	

Table 4: *Same as tab. 3, but with $\beta = 0.74603$.*

R	$N_t = 10$	$N_t = 12$	$N_t = 16$	$N_t = 24$
8	0.91749(14)	0.88387(10)	0.83207(8)	0.75075(7)
12	0.92941(16)	0.89646(12)	0.84523(9)	0.76492(8)
16	0.93597(17)	0.90351(14)	0.85220(10)	0.77193(8)
20	0.93999(18)	0.90723(14)	0.85655(12)	0.77661(9)
24	0.94292(19)	0.91074(16)	0.85937(13)	0.77926(10)
32	0.94706(21)	0.91444(18)	0.86371(16)	0.78311(11)
40	0.94864(20)	0.91717(18)	0.86624(15)	0.78532(12)
48	0.95111(23)	0.91875(20)	0.86740(17)	0.78677(13)

Table 5: *Same as tab. 3, but with $\beta = 0.75180$.*

N_t	z	$Q_1 \times 10^2$	$F^{NLO} \times 10^2$	$F^{free} \times 10^2$
7	6.857	-7.63(3)	-7.70(2)	-5.439
8	6.000	-6.15(3)	-6.05(3)	-4.504
9	5.333	-4.93(2)	-4.89(3)	-3.777
10	4.800	-4.12(2)	-4.03(3)	-3.195
11	4.364	-3.46(2)	-3.36(4)	-2.719
12	4.000	-2.93(2)	-2.83(4)	-2.322
14	3.428	-2.09(2)	-2.04(5)	-1.699
16	3.000	-1.53(2)	-1.46(5)	-1.232
18	2.667	-1.08(2)	-1.05(6)	-0.678
24	2.000	-0.31(2)	-0.24(8)	-0.140

Table 6: Results at $\beta = 0.74603$, with $R = 24$ kept fixed. In the first column the value of N_t that we simulated. In the second column the corresponding values of z , in the third, the values of Q_1 obtained from the simulations. In the fourth column the prediction for Q_1 with the first correction due to the Nambu-Goto action. In the last column the corresponding quantity obtained with the pure free bosonic string. These data are plotted in fig. 6.

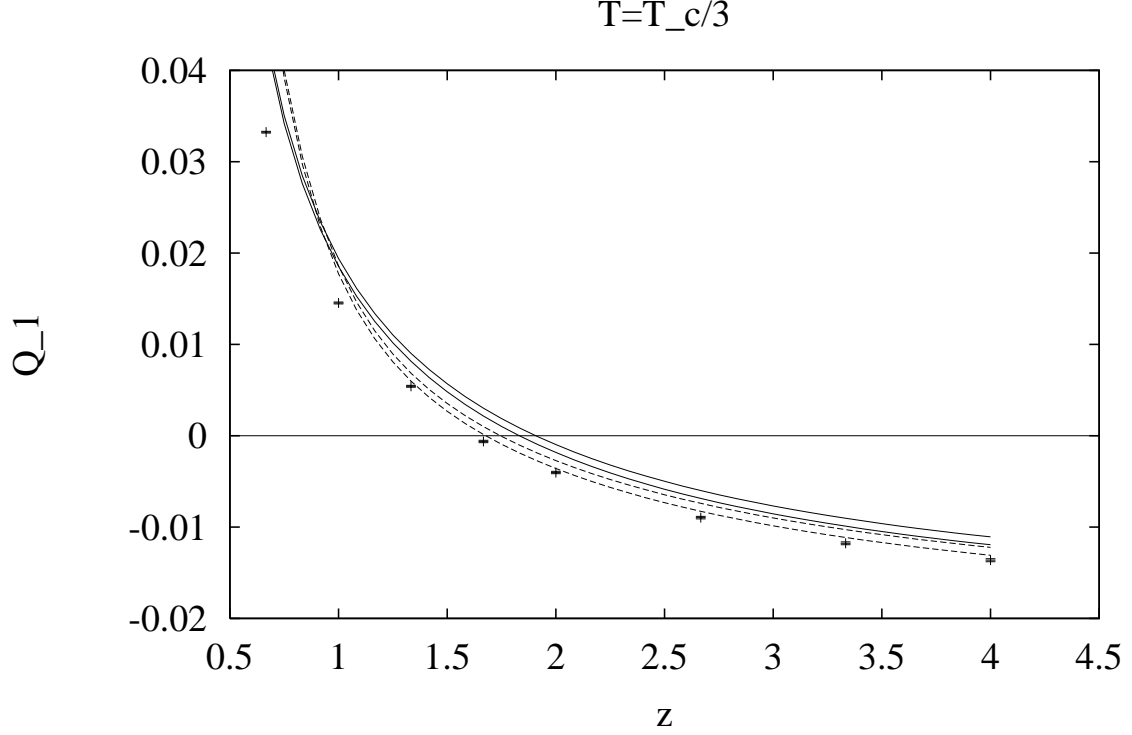


Figure 2: Q_1 for $N_t = 24$ (i.e. $T = T_c/3$) at $\beta = 0.75180$. The variable z is defined as $z \equiv \frac{2R}{N_t}$. The continuous lines correspond to the free bosonic string prediction, while the two dashed lines correspond to the first Nambu-Goto correction. The difference between the two dashed and the two continuous lines keeps into account the uncertainty in our estimate of σ . The pure area law corresponds to the line $Q_1 = 0$. The threshold $z_c = 2R_c/N_t$ beyond which the effective string picture is expected to hold is located at $z_c \sim 1$ for these values of N_t and β .

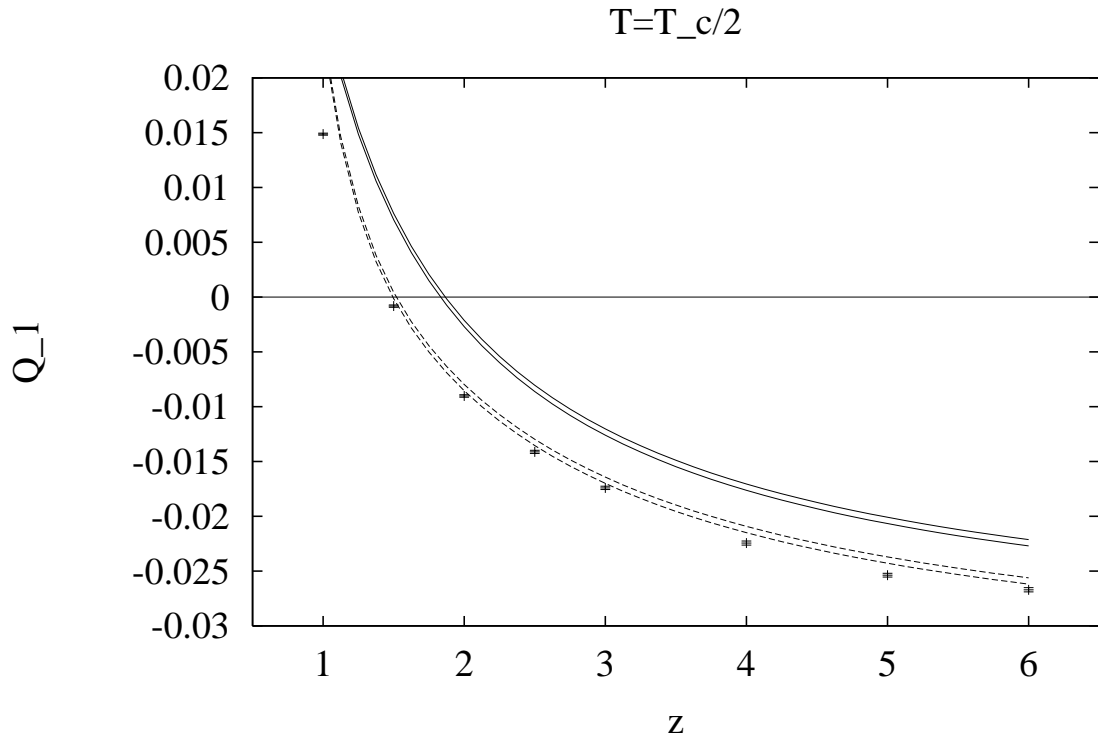


Figure 3: Same as fig. 2, but for $N_t = 16$ (i.e. $T = T_c/2$) at $\beta = 0.75180$. In this case we have $z_c \sim 1.5$.

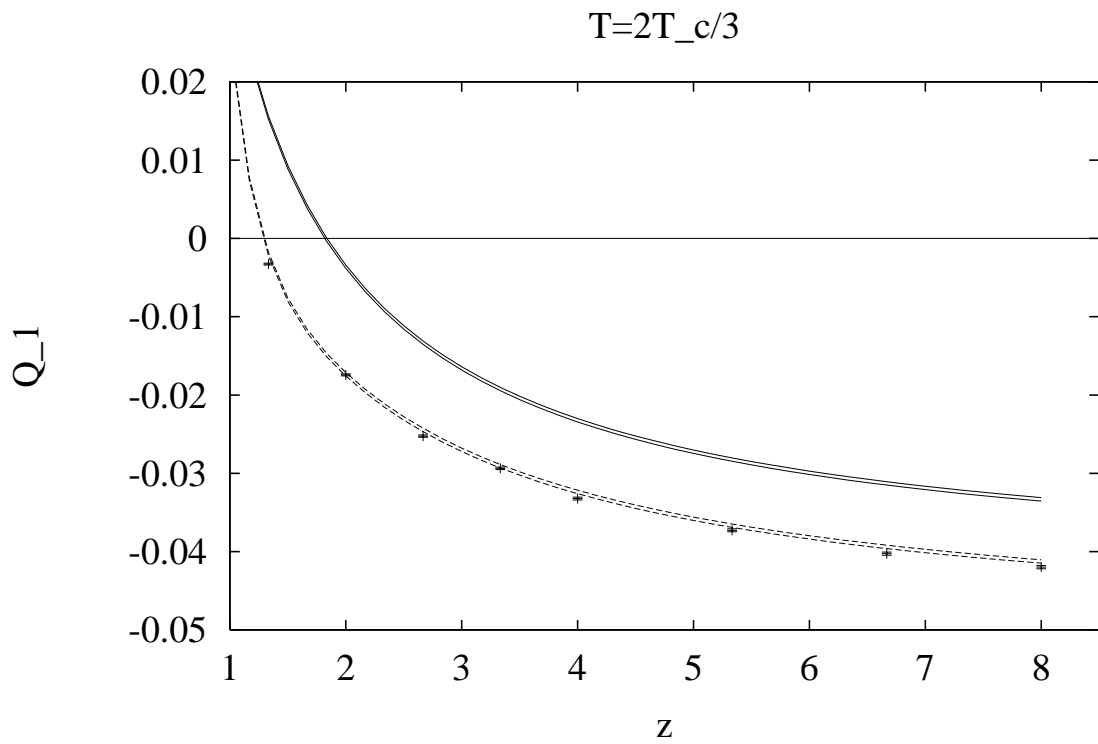


Figure 4: Same as fig. 2, but for $N_t = 12$ (i.e. $T = 2T_c/3$) at $\beta = 0.75180$. In this case we have $z_c \sim 2$.

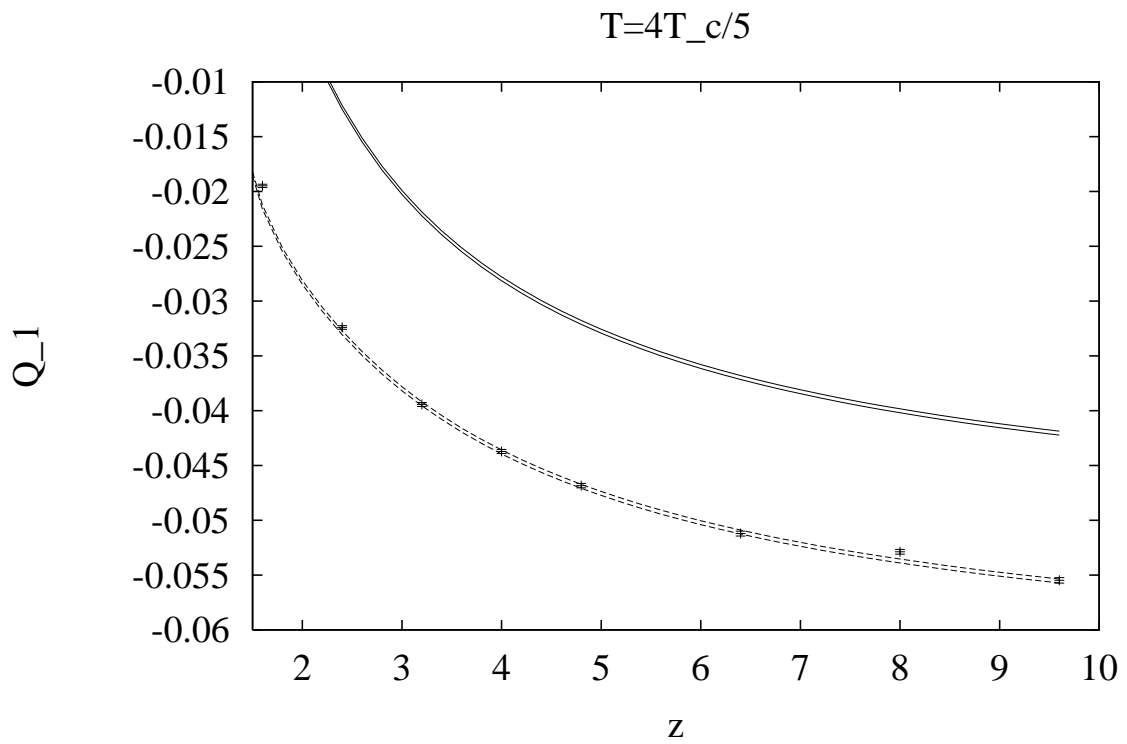


Figure 5: Same as fig. 2, but for $N_t = 10$ (i.e. $T = 4T_c/5$) at $\beta = 0.75180$. In this case we have $z_c \sim 2.4$.

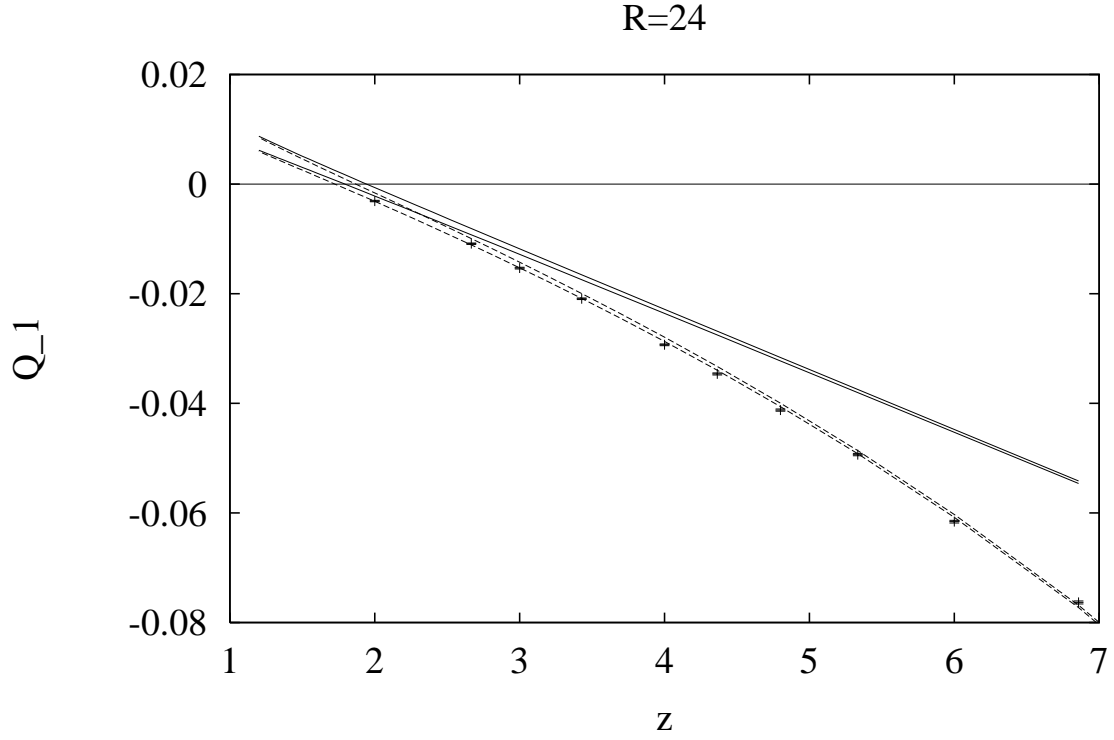


Figure 6: Q_1 for $R = 24$ and the values of N_t reported in tab. 3 at $\beta = 0.74603$. As in the previous figures the continuous lines correspond to the free string prediction while the two dashed lines correspond to the first Nambu-Goto correction. For this value of β we have $R_c = 9$.

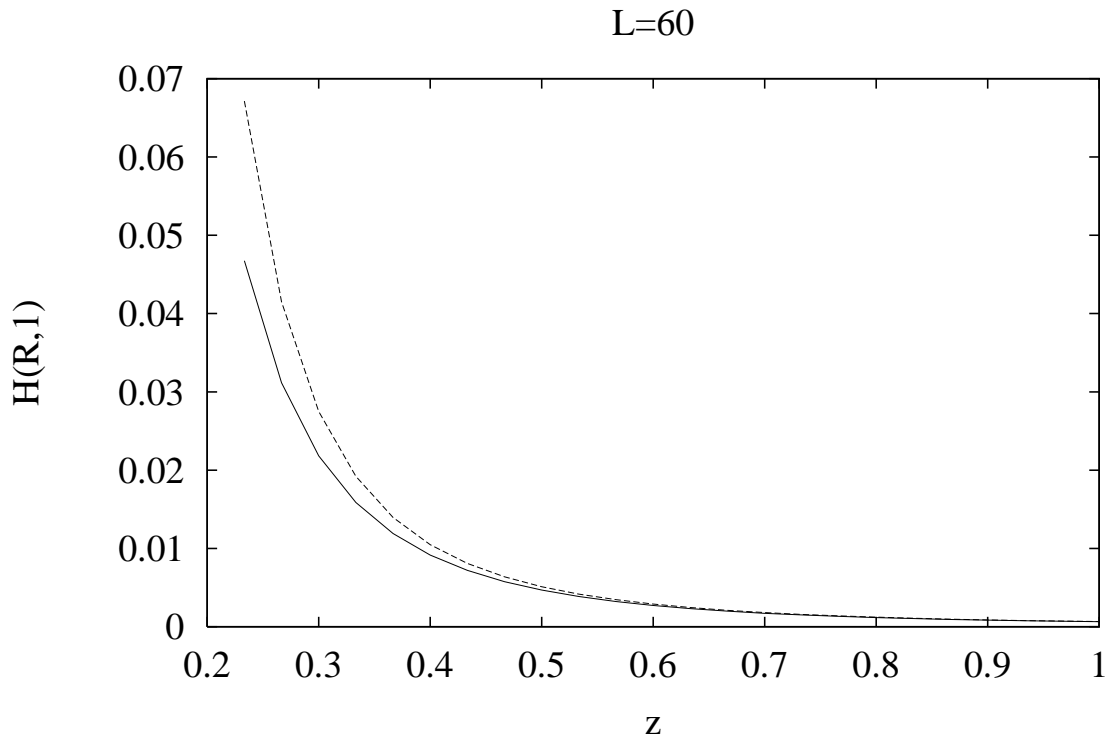


Figure 7: $H(R, 1)$ as a function of z for an hypothetical sample with $L = 60$ and R ranging from 6 to 30 (i.e. $z < 1$). The continuous line is the pure bosonic string correction, while the dashed line denotes the Nambu-Goto one.

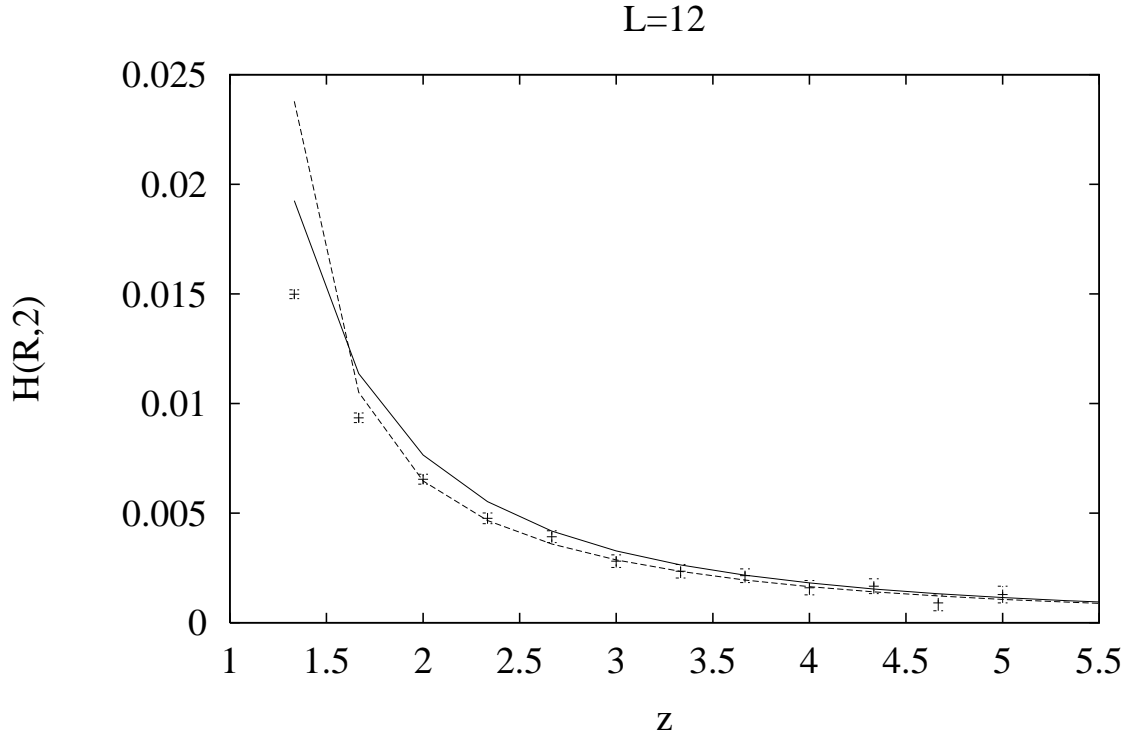


Figure 8: $H(R, 2)$ for the data at $\beta = 0.74603$ and $N_t = 12$. The continuous line is the pure bosonic string correction, while the dashed line denotes the Nambu-Goto one. For this sample $z_c \sim 1.5$.